H19/miR-194/E2F3 regulating loop promotes gastric cancer growth and metastasis

Wanxiang Qin
Army Medical University

Ying Shi
Army Medical University

Dan Zhu
Army Medical University

Yaohua Chen
Army Medical University

Yuping Li
Army Medical University

Jian Cui
Army Medical University

Research article

Keywords: LncRNA, H19, MicroRNA, CeRNA, MiR-194, E2F3, Gastric cancer

Abstract

Background

Gastric cancer (GC) is one of the most frequent malignant digestive tumors and second fatal cancer. This study was to investigate whether lncRNA-H19 can regulate E2F3 expression through competitive binding to microRNA-194 (miR-194), thus regulating GC growth and metastasis.

Methods

H19, miR-194, and E2F3 expression levels in GC tissues and cell lines were investigated using quantitative reverse transcriptase-polymerase chain reaction (QRT-PCR). Meanwhile, the mRNA levels of H19 and E2F3 in gastric cancer tissues were also analyzed through the GEPIA web tool. The binding condition of miR-194 with H19 and E2F3 was investigated using a dual-luciferase reporter gene assay. The regulatory effects of H19 on proliferative, migratory, and invasive abilities of AGS cells and SGC-7901 cells were detected by transwell assay and cell counting kit-8 (CCK-8). Genes involved in proliferation, migration, and invasion (PCNA, Vimentin, and N-cadherin) were determined using QRT-PCR. The regulatory interaction between H19 and miR-194, miR-194, and E2F3 were investigated using rescue experiments.

Results

The results revealed that H19 was highly expressed in GC tissues and cell lines than those of controls. Downregulated H19 decreased the proliferation, migration, and invasion of AGS cells and SGC-7901 cells. H19 was demonstrated that being the molecular sponge of miR-194 in regulating the growth of the GC cells. The level of E2F3 expression was also found significantly higher in GC tissues and cell lines than those of controls. And then, the mimics of miR-194 inhibited the expression of E2F3 in the GC cells. CCK-8 assay showed decreased proliferative ability induced by miR-194 mimics were reversed by E2F3 overexpression. Transwell assays showed decreased migratory and invasive ability induced by miR-194 mimics were reversed by E2F3 overexpression.

Conclusions

This study demonstrates that H19 promotes GC growth and metastasis by regulating E2F3 via competitive binding to miRNA-194.

Background

Gastric cancer (GC) is one of the most frequent malignant digestive tumors [1,2]. Over the past decades, although significant progress has been made, the overall 5-year survival rate of GC patients remains poor[3]. It is urgent to explore the underlying molecular mechanisms of GC and to discover effective therapeutic approaches for GC.

Non-coding RNAs (ncRNAs) account for 98% of human transcriptome. Numerous studies demonstrated that microRNAs (miRNAs) participate in almost all important cellular biological processes and can act as onco-miRNAs or tumor suppressors[4]. Long non-coding RNAs (lncRNAs), a subtype of ncRNAs, which role in cancer development has received increasing attentions[5]. LncRNAs, with no protein-coding capacity, have more than 200 nucleotides in length[6]. LncRNAs have been reported play a pivotal role in cancer cell proliferation, metastasis, and invasion, which also have been confirmed that they participated in the carcinogenesis of different cancer type[7]. Therefore, it might be necessary to investigate the mechanism of lncRNAs in tumor progression and to seek novel therapeutic strategies and biomarkers.

In the current study, we recruited several functional assays to determine the role of H19, a highly conservative lncRNA, in GC. Bioinformatics analysis and QRT-PCR assay were used to detect the level of lncRNA-H19 expression in GC. The results showed that the level of lncRNA-H19 expression was significantly higher in GC tissues and cell lines than that in control. Bioinformatics databases (http://www.mirdb.org and http://mirtarbase.mbc.nctu.edu.tw/php/index.php) and (http://starbase.sysu.edu.cn/starbase2/) indicated that H19 could directly bind to microRNA−194(miR−194), and E2F transcription factor 3 (E2F3) as possible target genes for miR−194. This study is to better understand the regulatory role of the H19/miR−194/E2F3 loop in the gastric carcinogenesis.

Materials And Methods

Sample Information

A total of 30 pairs of GC tissues and para-carcinoma normal tissues were obtained in this study. And GC tissue included 21 metastatic-positive and nine metastatic-free cases. Enrolled patients were pathologically diagnosed as GC.

The Online Database Gene Expression Profiling (the GEPIA web tool)

Based on The Cancer Genome Atlas (TCGA) and the Genotype-Tissue Expression (GTEx) projects, the RNA sequencing expression data related to our project was analyzed using the GEPIA web tool (http://gepia.cancerpku.cn/index. html.).

Cell culture and transfection

The gastric cancer cell lines (SGC−7901, SUN−16, MKN−45, and AGS cells) and the human gastric epithelial cell line GES−1 (American Type Culture Collection, USA) were used in this study. All cells cultured respectively in Dulbecco's Modified Eagle Medium (DMEM, Gibco, USA) supplemented with 10% fetal bovine serum (FBS), 100 U/mL penicillin and 100 μg/mL streptomycin (Hyclone, USA) and incubated in a 5% carbon oxide (CO_2) incubator at 37°C.

For cell transfection, cells in logarithmic growth phase were transfected with corresponding constructs when the confluence was up to 80% following the instructions of Lipofectamine2000 (Invitrogen, USA). The culture medium was replaced 6 hours later. H19-small interfering RNA (si-H19), miR−194 mimic, miR−194 inhibitor, pcDNA-E2F3, and negative control (NC) were constructed by Gene Pharma (Shanghai, China).

Luciferase reporter assay

Luciferase assay was used to investigate the interaction among H19, miR−194, and the target gene E2F3 with a Dual-Luciferase Reporter Assay System (Promega, USA). The 3'UTR sequence of H19 and E2F3 were downloaded from the National Center for Biotechnology Information (NCBI, USA) for the construction of wild-type H19 (H19-WT), wild-type E2F3 (E2F3-WT) and mutant-type H19 (H19-MUT), mutant-type E2F3 (E2F3-MUT). AGS cells were co-transfected with 50 pmol/L miR−194 mimic (or NC) and 80 ng of H19 WT (or E2F3-WT) or H19 MUT (or E2F3-MUT), respectively. Luciferase activity was detected after transfection for 48 hours.

Cell counting kit−8 (CCK−8) assay

For determining the proliferative ability of GC cells, the transfected cells were incubated in 100 μl culture medium each well (6×10^3 cells/well) using 96-well plates. At different set time, the CCK−8 solution (Beyotime, Shanghai, China) (10 μL/well) was added to cells and then incubated at 37°C for 2 hours in the dark. The optical density (OD) value (450 nm) was evaluated by a microplate reader.

Cell migration and invasion assays

Transwell assay was used to investigate the migration and invasion of GC cells. Different group GC cells were put on the upper Matrigel-coated invasion chambers or non-coated migration chambers (BD Biosciences, USA), respectively. 500 μl of DMEM medium containing 10% FBS was put in the lower chamber, and serum-free medium was put in the upper chamber. The non-invasive cells were wiped off by cotton swabs after 48 hours of incubation. The migrating and invading cells were fixed with 95% ethanol, stained with 0.1% crystal violet. The number of migratory and invasive cells in the lower chamber were counted under an inverted microscope (×100). The experiments were independently repeated for three times.

Western blotting

The total protein of treated cells was extracted using a radioimmunoprecipitation assay (RIPA) kit (Beyotime, China). The sample of protein was separated by electrophoresis on 10% sodium dodecyl sulfate-polyacrylamide gel electrophoresis (SDS-PAGE) and then transferred to polyvinylidene difluoride

(PVDF) membrane (Millipore, USA). Followed by the blocks with skimmed milk, the membranes were incubated with primary antibodies (Cell Signaling Technology, USA) overnight at 4°C. After being washed with Tris-buffered Saline with Tween 20 (TBS-T) for three times, the membranes were incubated with secondary antibody at 24°C for 1 hour. The protein blot on the membrane was exposed by chemiluminescence.

QRT-PCR

The total RNA was extracted from the ASCs with an RNeasy Mini Kit and then transcribed reversely with a SuperScript III kit (Invitrogen, CA). QRT-PCR was performed with a polymerase chain reaction instrument (Opticon CFD−3200, MA). The primer sets included: H19: forward, GCCGAGTTCGCTAGGCAAGCA; reverse, CTCAACTGGTGTCGTGGA. miR−194: forward, ACAGCAACTCCATGTGG; reverse, GAACATGTCTGCGTATCTC. E2F3: forward, AGCGGTCATCAGTACCTCTCAG; reverse, TGGTGAGCAGACCAAGAGACGT. PCNA: forward, CAAGTAATGTCGATAAAGAGGAGG; reverse, GTGTCACCGTTGAAGAGAGTGG. Vimentin: forward, CCTCCAGAGTTTACTGCCATGAC; reverse, GTAGGATCTCCGCCACTGATTC. N-cadherin: forward, AGGCAAAGCAGGAGTCCACTGA; reverse, ATCTGGCGTTCCAGGGACTCAT. β-actin: - forward, TCAGGTCATCACTATCGGCAAT; reverse, AAAGAAAGGGTGTAAAACCA. The relative expression of amplified RNA samples was calculated using the $2^{-\Delta\Delta CT}$ method, and β-actin was used as internal control. All experiments were done in triplicate.

Statistical analysis

All numerical data were expressed as the mean ±standard error of mean (SEM), and qualitative data were expressed as n (%). A comparison between the treatment groups of numerical data was analyzed by independent *t*-tests or 1-way or repeated-measures analysis of variance (ANOVA). Comparison between the treatment groups of qualitative data were analyzed by *chi-square* tests, and Fisher's exact tests were used for correction if necessary. All *p*-values were 2-tailed, and *p*-values less than 0.05 were considered statistically significant. For all statistical calculations, *p*-values were determined using SPSS (version 18.0 for Windows; SPSS, Inc., USA).

Results

H19 was overexpressed in GC tissues and cell lines

Using QRT-PCR assay, the expression level of H19 in GC tissues was found significantly higher than that in para-carcinoma normal tissues (Figure 1A). Consistently, the expression level of H19 was also significantly higher in GC cell lines than that in gastric epithelial cell line GES−1 (Figure 1D). Moreover, the expression level of H19 in metastatic-positive GC tissues was significantly higher than that in metastatic-free GC tissues (Figure 1B). Meanwhile, through the GEPIA web tool, the mRNA levels of H19 was also found significantly upregulated in GC tissues, which was consistent with our results (Figure 1C).

H19 regulated the proliferation, migration, and invasion of GC cells

To further explore the function of H19 in GC cells, H19 was down-regulated by si-H19 in SGC−7901 cells (Figure 2A) and AGS cells (Figure 2C). The CCK8 showed that si-H19 significantly decreased the proliferative ability of SGC−7901 cells (Figure 2B) and AGS cells (Figure 2D). The QRT-PCR showed that si-H19 significantly decreased the expression levels of PCNA of AGS and SGC-7901 cells (Figure 2E). Transwell assays were used to detect the cell invasive and migratory abilities in si-H19-transfected GC cells, and si-H19 transfected GC cells exhibited a decreased invasion capacity (Figure 3A and 3C) and in migratory capacity (Figure 3B and 3D). The QRT-PCR showed that si-H19 significantly decreased the expression levels of EMT-associated molecules (Vimentin and N-cadherin) of AGS and SGC-7901 cells (Figure 3E and 3F). Meanwhile, the Overexpression of H19 promotes the PCNA and N-cadherin expression of GC cells in vitro(Figure 4D and 4E). These findings indicated that H19 promoted GC cell proliferation, migration, and invasion.

H19 was the molecular sponge of miR−194 in regulating the proliferation, migration, and invasion of GC cells

The putative binding site between miR−194 and H19 was predicted by bioinformatics (TargetScan, http://www.targetscan.org/) and screened out. H19 WT and H19 MUT plasmids were constructed (Figure 3A). The level of miR−194 mRNA was significantly inhibited in GC cell lines (Figure 3B). Luciferase reporter gene assay demonstrated that miR−194 overexpression led to a significant decrease in luciferase activity of pMIR-H19-WT, but not in pMIR-H19-MUT in AGS cells (Figure 3C). Moreover, the mRNA level of H19 was remarkably reduced after microRNA−194 mimics transfection in GC cells (Figure 3D). The above data indicated that H19 was the molecular sponge of miR−194.

CCK−8 assay showed decreased proliferative ability induced by si-H19 transfection were reversed by miR−194 knockdown in CGS−7901 cells (Figure 3E) and AGC cells (Figure 3F). Transwell assays showed decreased migratory ability (Figure 3G) and invasive ability (Figure 3H) induced by si-H19 transfection were reversed by miR−194 knockdown.

E2F3 was the functional target of miR−194 that affect proliferation, migration, and invasion of GC cells

To further study the mechanism of H19/miR−194 in GC cells, bioinformatics analysis (TargetScan, http://www.targetscan.org/) was used to determine the binding sites of miR−194 matched the 3'UTR of E2F3, which was also further confirmed by luciferase reporting assay. H19 WT and H19 MUT plasmids were constructed (Figure 4A). After 24 hours of transfection, we observed that over-expression of miR−194 led to a significant decrease in the Luciferase activity of the E2F3-wild group, but not in the E2F3-mutant group (Figure 4B). Moreover, the expression level of E2F3 protein was remarkably reduced after

miR−194 mimics transfection in GC cells (Figure 4E). All of these indicated that E2F3 was the direct target of miR−194.

The level of E2F3 mRNA was significantly up-regulated in GC cell lines (Figure 3D). Meanwhile, the levels of E2F3 mRNA were also found significantly up-regulated in GC tissues by using the GEPIA web tool (Figure 4B). CCK−8 assay showed decreased proliferative ability induced by miR−194 mimics were reversed by E2F3 overexpression in CGS−7901 cells (Figure 4F) and AGS cells (Figure 4G). Transwell assays showed decreased migratory ability (Figure 4H), and invasive ability (Figure 4I) induced by miR−194 mimics were reversed by E2F3 overexpression.

Discussion

In the present study, the level of H19 was firstly found significantly overexpressed in GC tissues and cell lines. Moreover, miR−194 and E2F3 were demonstrated being the downstream target of H19 and mediated the proliferation, migration, and invasion of GC cells (Figure 5).

Non-coding RNAs, one of the main mechanisms of epigenetics, do not exert the protein-encoding function. Abundant evidences have demonstrated that non-coding RNAs exert a vital role in epigenetic regulation. LncRNAs belong to non-coding RNAs with relatively long chains. It is reported that lncRNA expression is closely related to tumor development[8]. Disordered lncRNAs have an important effect on cellular homeostasis[9]. H19 is located on human chromosome 11p15.5. Studies have found that H19 is overexpressed in various malignancies, which indicated that H19 overexpression could upregulate the proliferation of tumor cells and promote tumor cell migration and invasion[11, 12].

Based on the Starbase database (http://starbase.sysu.edu.cn/starbase2/), miR−194 was manifested being the direct target of H19. And in our study, dual-luciferase reporter gene assay demonstrated that H19 could directly bind to miR−194. miR−194 is one of the tumor suppressor miRNAs[13], which specifically expressed in the gastrointestinal tract, and was aberrantly expressed within diversified malignant neoplasms, including GC[14]. And our data showed that H19 was the molecular sponge of miR− 194 in regulating the proliferation, migration, and invasion of GC, which is consistent with previous researches indicated that miR−194 was down-regulated in cancer[15, 16].

Moreover, the Bioinformatics method and luciferase activity assay were performed to confirm that miR− 194 directly target at E2F3. Also, western blot results showed that the miR−194 mimics could significantly decrease the protein expression level of E2F3 in the GC cells. E2F3 is one of the key members of the E2F family[17], which has an important role in cell cycle[18] and controls gene expression related to cell cycle during the G1/S transition[19]. E2F3 may function as an oncogene in GC[20, 21]. Previous studies have reported that overexpression of E2F3 is a frequent oncogenic event in human tumorigenesis and that this may be regulated by miRNA[22, 23]. In this study, the expression level of E2F3 was found significantly overexpressed in GC cell lines, which was consistent with the data of GC tissues in the GEPIA web tool (http://gepia.cancer-pku.cn). And CCK−8 assay showed decreased proliferative ability induced

by miR−194 mimics were reversed by E2F3 overexpression in CGS−7901 cells and AGC cells. Transwell assays showed decreased migratory and invasive ability induced by miR−194 mimics were also reversed by E2F3 overexpression. All of these indicated that E2F3 was the functional targets of H19/miR−194 that affect proliferation, migration, and invasion of GC cells.

Conclusions

In conclusion, the major findings of this study can be summarized as follows: (1) H19 was significantly upregulated in GC tissues and cell lines. (2) H19 promoted GC cell proliferation, migration, and invasion. (3) H19 was the molecular sponge of miR−194 in regulating the proliferation, migration, and invasion of GC cells. (4) H19/miR−675 modulates gastric cancer progression by targeting E2F3. Thus, our study provides valuable clues for understanding the regulatory network of H19 in carcinogenesis and identifying new therapeutic targets for the treatment of gastric cancer.

Abbreviations

miR−194: microRNA−194; GC: gastric cancer; qRT-PCR: quantitative reverse transcriptase-polymerase chain reaction; CCK−8: cell counting kit−8; ncRNAs: Non-coding RNAs; miRNAs: microRNAs; lncRNAs: Long non-coding RNAs; TCGA: The Cancer Genome Atlas; GTEx: Genotype-Tissue Expression; DMEM: Dulbecco's Modified Eagle Medium; FBS: fetal bovine serum; CO2: Carbon dioxide; si-H19: H19-small interfering RNA; NC: negative control; H19-WT: wild-type H19; E2F3-WT: wild-type E2F3; H19-MUT: mutant-type H19; E2F3-MUT: mutant-type E2F3; OD: optical density; RIPA: radioimmunoprecipitation assay; SDS-PAGE: sodium dodecyl sulphate-polyacrylamide gel electrophoresis; PVDF: polyvinylidene difluoride; TBS-T: Tris-buffered Saline with Tween 20; QRT-PCR: Quantitative Real-Time Reverse Transcription Polymerase Chain Reaction; SD: standard deviation; ANOVA: 1-way or repeated-measures analysis of variance.

Declarations

Ethics, consent, and permissions

This study was approved by the Research Ethics Committee in Southwest Hospital, and informed consent of all patients was obtained.

Consent for publication

Verbal consent was obtained from all participants in this article, and the participants agree for publication.

Availability of data and materials

The data that support the findings of this study are available on request from the first or corresponding author.

Competing interests

The authors declare that they have no competing interests.

Funding

This work was supported in part by the National Natural Science Foundation of China (No. 81870883) and a clinical innovation program of Southwest Hospital (No. SWH2016YSCXYB–14). The funding body did not participate in the design of this study, collecting, analyzing, and interpreting data and writing manuscripts.

Authors' contributions

WXQ was the principal investigator and mainly wrote a manuscript. YS, ZD, YHC, and YPL conducted experiments and data analysis. JC designed the experiments and supervised the manuscript. All authors read and approved the final manuscript.

Acknowledgments

The authors would like to thank the patients and the surgeons in the Department of General Surgery, Southwest Hospital, China, for their support in collecting the sample.

References

1) Chivu-Economescu M, Matei L, Necula LG, Dragu DL, Bleotu C, Diaconu CC. New therapeutic options opened by the molecular classification of gastric cancer. World J Gastroenterol 2018; 24(18):1942–1961.

2) Bray F, Ferlay J, Soerjomataram I, Siegel RL, Torre LA, Jemal A. Global cancer statistics 2018: GLOBOCAN estimates of incidence and mortality worldwide for 36 cancers in 185 countries. CA Cancer J Clin 2018; 68(6):394–424.

3) Li JF, Li WH, Xue LL, Zhang Y. Long non-coding RNA PICART1 inhibits cell proliferation by regulating the PI3K/AKT and MAPK/ERK signaling pathways in gastric cancer. Eur Rev Med Pharmacol Sci 2019; 23(2):588–597.

4) McLean MH, El-Omar EM. Genetics of gastric cancer. Nat Rev Gastroenterol Hepatol 2014; 11(11):664–674.

5) Chen X, Chen Z, Yu S, Nie F, Yan S, Ma P, Chen Q, Wei C, Fu H, Xu T, Ren S, Sun M, Wang Z. Long Noncoding RNA LINC01234 Functions as a Competing Endogenous RNA to Regulate CBFB Expression by Sponging miR−204−5p in Gastric Cancer. Clin Cancer Res 2018; 24(8):2002−2014.

6) Bartonicek N, Maag JL, Dinger ME. Long noncoding RNAs in cancer: mechanisms of action and technological advancements. Mol Cancer 2016; 15(1):43.

7) Perez DS, Hoage TR, Pritchett JR, Ducharme-Smith AL, Halling ML, Ganapathiraju SC, Streng PS, Smith DI. Long, abundantly expressed non-coding transcripts are altered in cancer. Hum Mol Genet 2008; 17(5):642−655.

8) Kotake Y, Nakagawa T, Kitagawa K, Suzuki S, Liu N, Kitagawa M, Xiong Y. Long non-coding RNA ANRIL is required for the PRC2 recruitment to and silencing of p15(INK4B) tumor suppressor gene. Oncogene 2011; 30(16):1956−1962.

9) Gutschner T, Diederichs S. The hallmarks of cancer: a long non-coding RNA point of view. Rna Biol 2012; 9(6):703−719.

10) Zhou QP, Zhang F, Zhang J, Ma D. H19 promotes the proliferation of osteocytes by inhibiting p53 during fracture healing. Eur Rev Med Pharmacol Sci 2018; 22(8):2226−2232.

11) Zhou X, Ye F, Yin C, Zhuang Y, Yue G, Zhang G. The Interaction Between MiR−141 and lncRNA-H19 in Regulating Cell Proliferation and Migration in Gastric Cancer. Cell Physiol Biochem 2015; 36(4):1440−1452.

12) Li C, Li Y, Wang Y, Sun L. The Effect of LncRNA H19/miR−194−5p Axis on the Epithelial-Mesenchymal Transition of Colorectal Adenocarcinoma. Cell Physiol Biochem 2018; 50(1):196−213.

13) Meng Z, Fu X, Chen X, Zeng S, Tian Y, Jove R, Xu R, Huang W. miR−194 is a marker of hepatic epithelial cells and suppresses metastasis of liver cancer cells in mice. Hepatology 2010; 52(6):2148−2157.

14) Li Z, Ying X, Chen H, Ye P, Shen Y, Pan W, Zhang L. MicroRNA−194 inhibits the epithelial-mesenchymal transition in gastric cancer cells by targeting FoxM1. Dig Dis Sci 2014; 59(9):2145−2152.

15) Zhu X, Li D, Yu F, Jia C, Xie J, Ma Y, Fan S, Cai H, Luo Q, Lv Z, Fan L. miR−194 inhibits the proliferation, invasion, migration, and enhances the chemosensitivity of non-small cell lung cancer cells by targeting forkhead box A1 protein. Oncotarget 2016; 7(11):13139−13152.

16) Zhao HJ, Ren LL, Wang ZH, Sun TT, Yu YN, Wang YC, Yan TT, Zou W, He J, Zhang Y, Hong J, Fang JY. MiR−194 deregulation contributes to colorectal carcinogenesis by targeting the AKT2 pathway. Theranostics 2014; 4(12):1193−1208.

17) Kent LN, Bae S, Tsai SY, Tang X, Srivastava A, Koivisto C, Martin CK, Ridolfi E, Miller GC, Zorko SM, Plevris E, Hadjiyannis Y, Perez M, Nolan E, Kladney R, Westendorp B, de Bruin A, Fernandez S, Rosol TJ, Pohar KS, Pipas JM, Leone G. Dosage-dependent copy number gains in E2f1 and E2f3 drive hepatocellular carcinoma. J Clin Invest 2017; 127(3):830–842.

18) Yang H, Wang L, Tang X, Bai W. miR–203a suppresses cell proliferation by targeting E2F transcription factor 3 in human gastric cancer. Oncol Lett 2017; 14(6):7687–7690.

19) Sharma N, Timmers C, Trikha P, Saavedra HI, Obery A, Leone G. Control of the p53-p21CIP1 Axis by E2f1, E2f2, and E2f3 is essential for G1/S progression and cellular transformation. J Biol Chem 2006; 281(47):36124–36131.

20) Li X, Li H, Zhang R, Liu J, Liu J. MicroRNA–449a inhibits proliferation and induces apoptosis by directly repressing E2F3 in gastric cancer. Cell Physiol Biochem 2015; 35(5):2033–2042.

21) Zhou X, Ji G, Ke X, Gu H, Jin W, Zhang G. MiR–141 Inhibits Gastric Cancer Proliferation by Interacting with Long Noncoding RNA MEG3 and Down-Regulating E2F3 Expression. Digest Dis Sci 2015; 60(11):3271–3282.

22) Oeggerli M, Tomovska S, Schraml P, Calvano-Forte D, Schafroth S, Simon R, Gasser T, Mihatsch MJ, Sauter G. E2F3 amplification and overexpression is associated with invasive tumor growth and rapid tumor cell proliferation in urinary bladder cancer. Oncogene 2004; 23(33):5616–5623.

23) Miles WO, Tschop K, Herr A, Ji JY, Dyson NJ. Pumilio facilitates miRNA regulation of the E2F3 oncogene. Genes Dev 2012; 26(4):356–368.

Figures
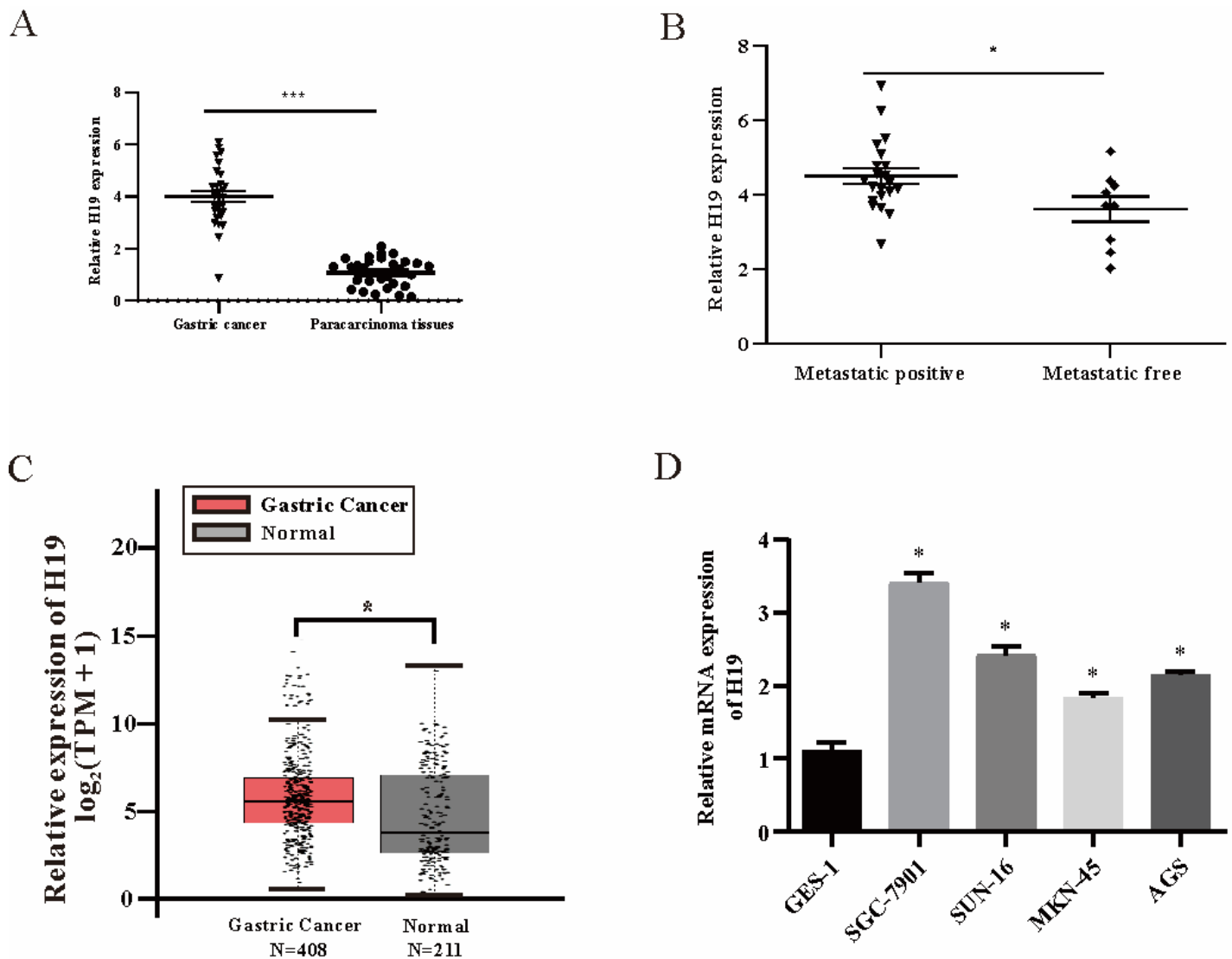
Figure 1

LncRNA-H19 was highly expressed in both GC tissues and cell lines. (A) The relative expression level of lncRNA-H19 in GC tissues and matched para-carcinoma normal tissues; (B) H19 expression was highly expressed in metastatic positive GC tissues than metastatic free tissues; (C) The GEPIA database revealed that H19 expression was significantly up-regulated in GC tissues. The boxplot analysis showed log2 (TPM + 1) on a log-scale; (D) Analysis of lncRNA-H19 expression level in GC cell lines. Data are presented as mean ± SEM; * p < 0.05.
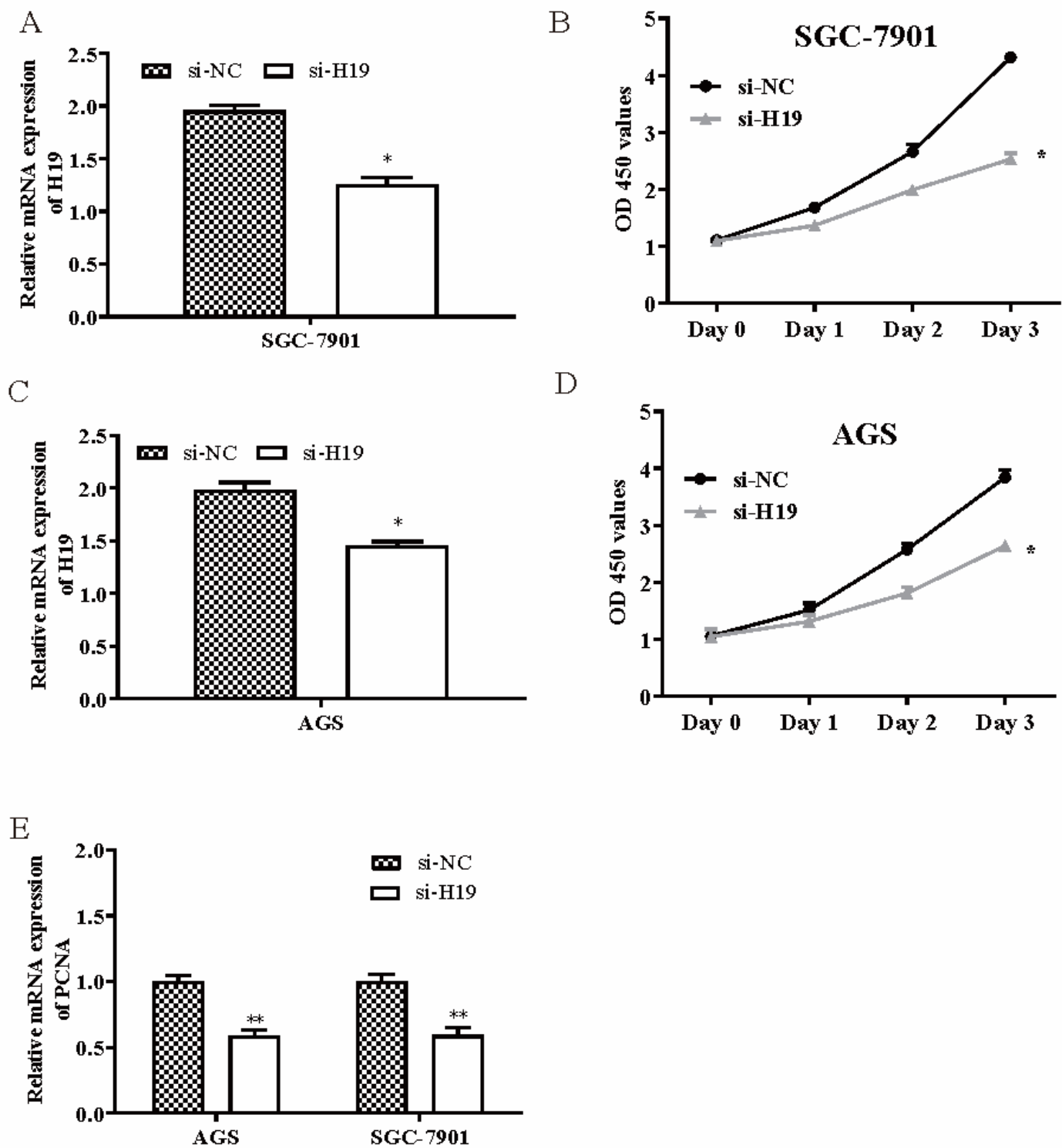
Figure 2

The downregulation of H19 suppresses the proliferation of GC cells in vitro. (A) Transfection efficacy of si-H19 in SGC-7901 cells. (B) CCK-8 assay showed decreased proliferative ability in SGC-7901 cells transfected with si-H19 compared with those transfected with si-NC. (C) Transfection efficacy of si-H19 in AGS cells. (D) CCK-8 assay showed decreased proliferative ability in AGS cells transfected with si-H19

compared with those transfected with si-NC. (E) The expression levels of PCNA in transfected AGS and SGC-7901 cells were determined using QRT-PCR. Data are presented as mean ± SEM; * p < 0.05.
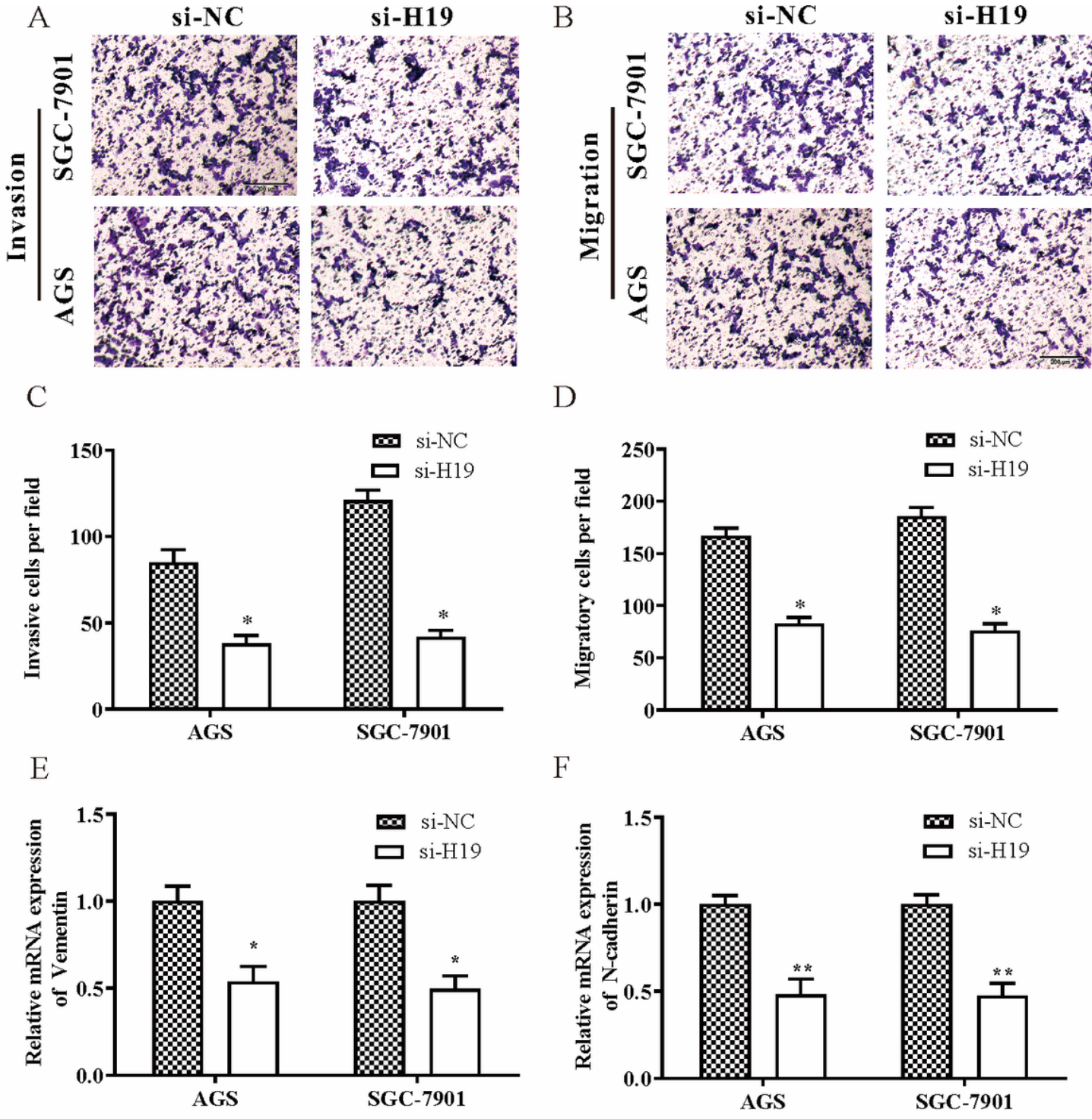
Figure 3

The downregulation of H19 suppresses the migration and invasion of GC cells in vitro. (A and C) Transwell invasion assays were used to determine the cell migration abilities in si-H19-transfected AGS cells or SGC-7901 cells. (B and D) Transwell migration assays were used to determine the cell migration abilities in si-H19-transfected AGS cells or SGC-7901 cells. (E and F) The expression levels of

EMT-associated molecules (Vimentin and N-cadherin) in transfected AGS and SGC-7901 cells were determined using QRT-PCR. Data are presented as mean ± SEM; * p < 0.05.
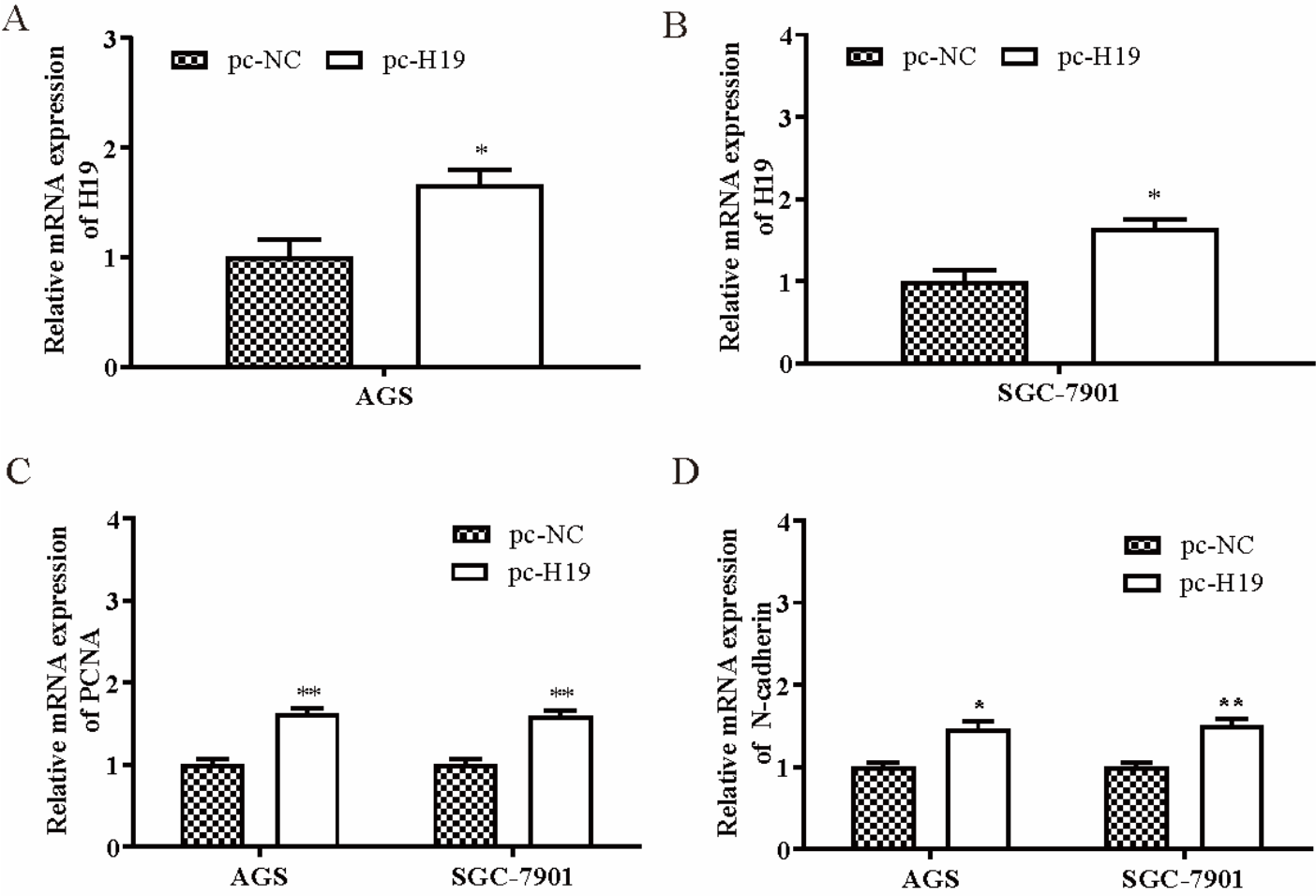
Figure 4

Overexpression of H19 promotes the PCNA and N-cadherin expression of GC cells in vitro. (A) Transfection efficacy of pc-H19 in AGS cells. (B) Transfection efficacy of pc-H19 in SGC-7901 cells. (C) The expression levels of PCNA in transfected AGS and SGC-7901 cells were determined using QRT-PCR. (D) The expression levels of N-cadherin in transfected AGS and SGC-7901 cells were determined using QRT-PCR. Data are presented as mean ± SEM; * p < 0.05.
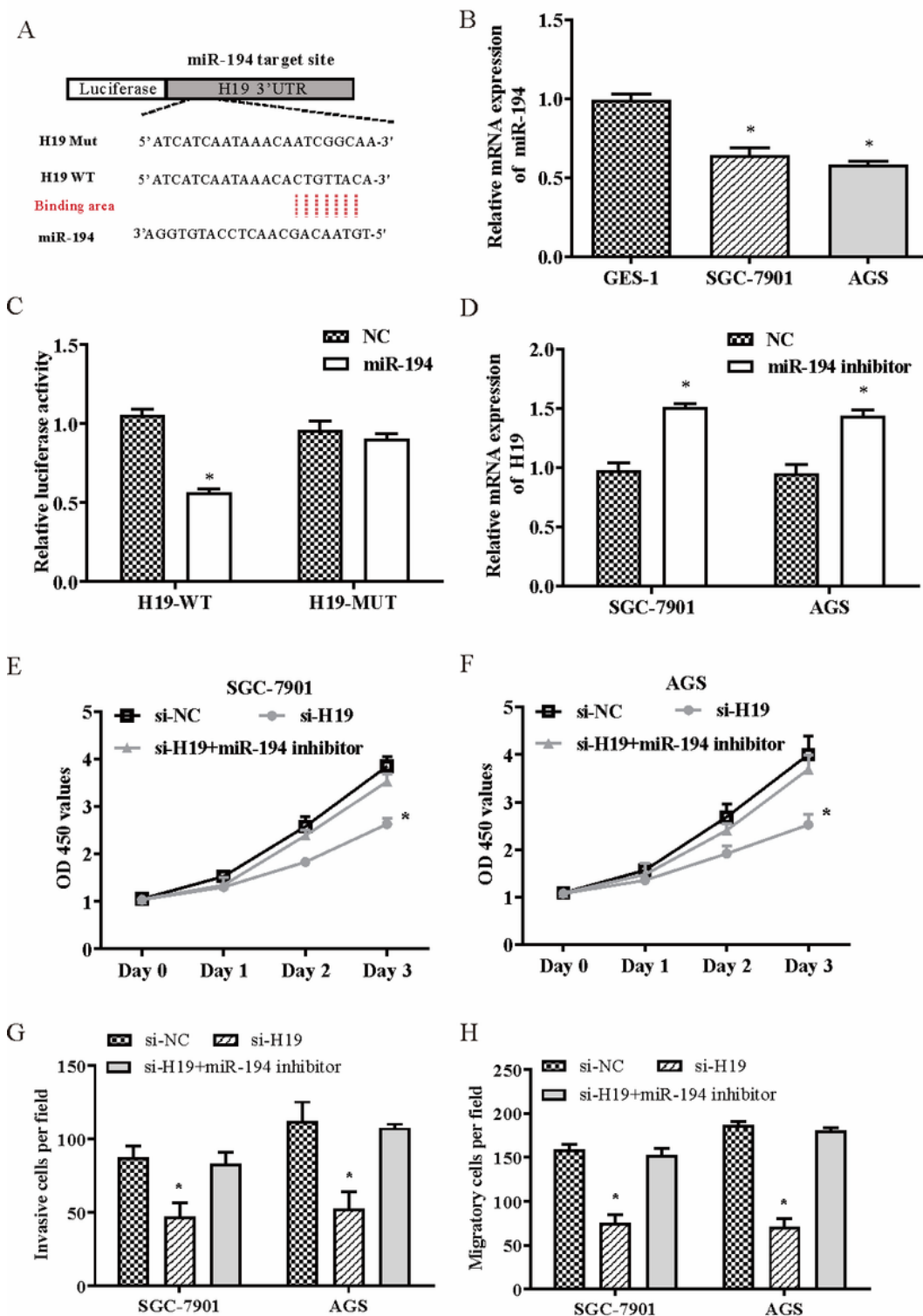
Figure 5

H19 was the molecular sponge of miR-194 and regulated proliferation and migration of GC cells. (A) The putative binding sites of miR-194 on H19, and H19 WT and H19 MUT plasmids were constructed. (B) Analysis of miR-194 expression level in GC cell lines. (C) Over-expression of miR-194 led to a marked decrease in luciferase activity of pMIR-H19-WT, without any change in luciferase activity of pMIR-H19-MUT in AGS cells. (D) The expression levels of H19 in GC cells transfected with the miR-194 inhibitor. (E)

CCK-8 assay showed decreased proliferative ability induced by si-H19 transfection were reversed by miR-194 knockdown in CGS-7901 cells. (F) CCK-8 assay showed decreased proliferative ability induced by si-H19 transfection were reversed by miR-194 knockdown in AGC cells. (G) Transwell migration assays showed decreased migratory ability induced by si-H19 transfection were reversed by miR-194 knockdown. (H) Transwell invasion assays showed decreased invasive ability induced by si-H19 transfection were reversed by miR-194 knockdown. Data are presented as mean ± SEM; * p <0.05.
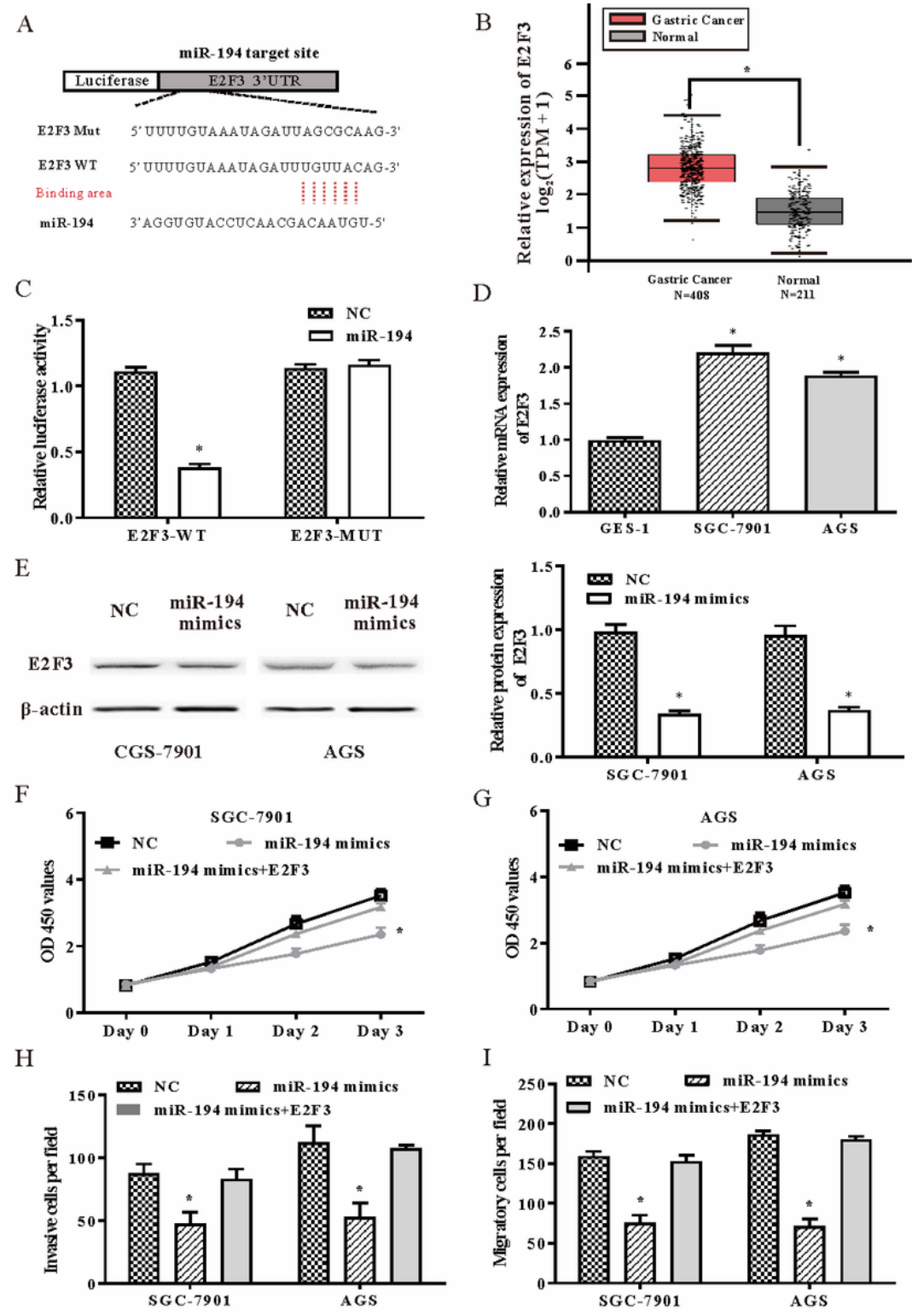
Figure 6

E2F3 was the functional targets of miR-194 that affect the proliferation and migration of GC cells. (A) The putative binding sites of miR-194 on E2F3, and E2F3 WT and E2F3 MUT plasmids were constructed. (B) The GEPIA database revealed that E2F3 expression was significantly upregulated in GC tissues. The boxplot analysis show log2 (TPM + 1) on a log-scale. (C) Over-expression of miR-194 led to a marked decrease in luciferase activity of pMIR-E2F3-WT, without any change in luciferase activity of pMIR-E2F3-MUT in AGS cells. (D) Analysis of lncRNA-H19 expression level in GC cell lines. (E) The Western blot showed protein expression levels of E2F3 in GC cells transfected with the miR-194 mimics or NC. (F) CCK-8 assay showed E2F3 plasmids reversed the effect of miR-194 on the proliferative ability of SGC-7901 cells. (G) CCK-8 assay showed E2F3 plasmids reversed the effect of miR-194 on the proliferative ability of AGS cells. (H) Transwell migration assays showed E2F3 plasmids reversed the effect of miR-194 on the migration ability of GC cells. (I) Transwell invasion assays showed E2F3 plasmids reversed the effect of miR-194 on the migration ability of GC cells. Data are presented as mean ± SEM; *Significant differences, p <0.05.
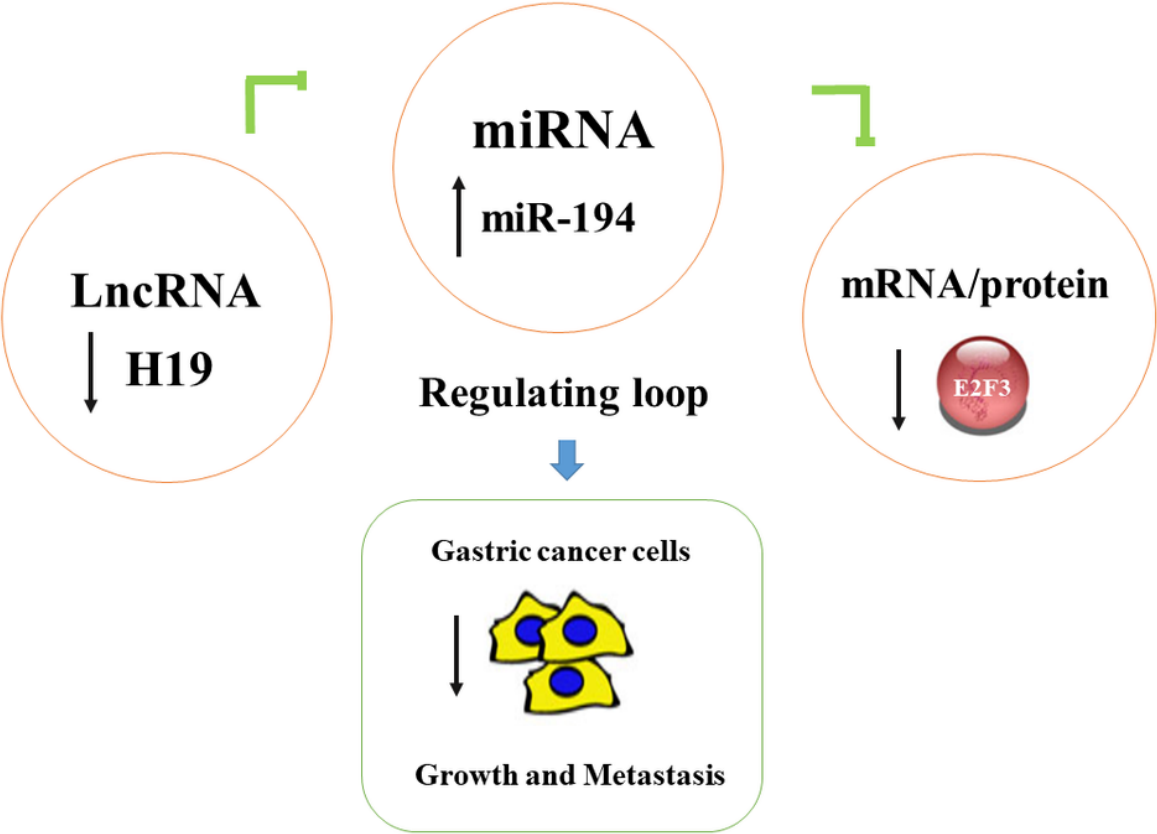
Figure 7

A proposed schematic diagram of H19/miR-194/E2F3 regulating loop promotes gastric cancer growth and metastasis.